

YBa₂Cu₃O_{7-x} 45° [001] Tilt Grain Boundaries Induced by Controlled Low-Energy Sputtering of MgO Substrates: Transport Properties and Atomic-Scale Structure

Boris V. Vuchic, Karl L. Merkle and Jeffrey W. Funkhouser
Materials Science Division, Argonne National Laboratory, Argonne, IL

D. Bruce Buchholz, Kenneth A. Dean, Robert P.H. Chang and Laurence D. Marks
Materials Science and Engineering Department, Northwestern University, Evanston, IL

Abstract --- Grain boundaries can act as weak links in the high T_c materials. If properly controlled, these grain boundaries can be used in various device applications. We have been able to reproducibly form 45° [001] tilt grain boundary junctions in YBa₂Cu₃O_{7-x} thin films. The films were grown on MgO substrates using a pre-growth substrate treatment. A low energy broad beam Argon ion source was used to irradiate a select region of (100) MgO substrates. The film on the milled portion of the substrate grows predominantly with a grain orientation rotated 45° about the c-axis with respect to the grain on the unmilled portion. Backscattered electron Kikuchi patterns have been used to confirm that the rotation occurs across the entire milled portion of the substrate. Transport properties of these films are discussed and related to high resolution electron microstructural and microchemical analyses of the grain boundaries. This technique has potential use in device applications as a method for controlled grain boundary engineering.

I. Introduction

Since the discovery of high-temperature superconductors, understanding and controlling grain boundary properties has been critical in the development of commercial high T_c applications. The first comprehensive study on grain boundaries showed that high-angle grain boundaries have reduced critical current densities relative to the grains [1], [2]. Weak link high-angle grain boundaries have been detrimental in high power, large critical current applications. Many device applications, however, rely on controlling the properties of the high-angle grain boundaries to create Josephson junctions. There have been various types of thin film grain boundaries used as junctions including bi-crystals [3], [4], bi-epitaxial junctions [5], [6] and step-edge junctions [7]. The major characteristics in making the

junctions commercially viable include, reproducibility of junction characteristics, planarization, flexibility of junction placement, high $I_c R_n$ values and simplicity of implementation.

Grain boundary junction properties are particularly hard to control due to difficulty in reproducing the grain boundary structure. There are several key issues involving grain boundary structure and composition which affect the properties. Microstructurally the key factors include meandering, local symmetry and second phases or amorphous phases at the grain boundary. The local chemistry is also important in determining the grain boundary properties due to oxygen deficiency and other impurities.

MgO is a common substrate for high- T_c thin films. Previous work has shown that ion beam modification could affect the epitaxial relation between a YBa₂Cu₃O_{7-x} thin film and a MgO substrate [8]. We have developed a technique to form 45° grain boundary junctions on MgO (100) substrates. This technique involves a low energy Argon ion sputter pre-treatment of the substrate prior to growing the YBa₂Cu₃O_{7-x} thin film using pulsed organo metallic beam epitaxy (POMBE). The thin film grown on the sputtered portion of the substrate is rotated 45° about [001] relative to the film grown on the unsputtered portion. The technique allows the placement of grain boundary junctions in virtually any configuration on the substrate. The grain boundary junctions created have well structured, uniform grain boundaries with favorable transport properties compared to other YBa₂Cu₃O_{7-x} 45° thin film grain boundaries.

II. Experimental

The substrates were commercially polished single crystal (100) MgO. A portion of the substrate was masked using either a metal contact mask or hardbaked photoresist (see figure 1). The sputtering was performed with a background pressure of 2×10^{-4} torr. A 3 cm diameter Kaufman-type Argon ion source was used with accelerating voltages from 100 eV to 500 eV. The ion beam current density was approximately 1 mA/cm^2 . The ions were incident on the substrate parallel to the surface normal. Irradiation times were 2 minutes or greater.

Manuscript received October 17, 1994

This work was supported by the National Science Foundation Office of Science and Technology Centers, under contract #DMR 91-20000 and the U.S. Department of Energy, Basic Energy Sciences-Materials Science, under contract #W-31-109-ENG-38.

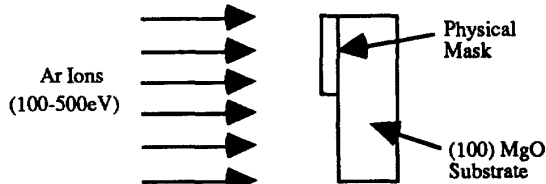


Fig. 1. Schematic diagram of (100) MgO substrate configuration during ion irradiation.

After the ion irradiation the mask was removed. The $\text{YBa}_2\text{Cu}_3\text{O}_{7-x}$ thin films were deposited *in situ* using POMBE which is described in detail elsewhere[9]. The samples are held at growth temperature (approximately 700°C) and in an oxygen plasma for 30 minutes prior to deposition. The $\text{YBa}_2\text{Cu}_3\text{O}_{7-x}$ is grown in an oxygen plasma to ensure full oxygenation. The ambient gas in the growth chamber during deposition was approximately 70% oxygen, 28% helium and 2% water vapor. The deposition rates of the films varied from 3Å/min to 11Å/min. The film thicknesses were between 2100Å and 3000Å. The POMBE technique relies upon the slow deposition rates and the oxygen plasma environment during growth. These two factors are integral in ensuring reproducibility and in forming well structured, clean grain boundaries.

The local crystallographic orientation of the thin film was determined using backscattered electron Kikuchi patterns in a JEOL 6400 scanning electron microscope. The samples were patterned with 35µm wide microbridges using Argon ion etching. Silver leads were evaporated *in-situ* after 500 eV Argon ion sputtering to ensure low contact resistances. The microbridge configuration allowed for separate measurement of the two grains on either side of the grain boundary junction as well as across the grain boundary. Voltage-current characteristics were measured as a function of temperature using a helium flow cryostat.

High resolution electron microscope samples were made using standard grinding, dimpling and ion milling techniques. High resolution electron microscopy was performed on a JEOL 4000 EXII at 200kV to minimize electron beam damage. A Hitachi HF-2000 with a low temperature stage was used for high spatial resolution analytical electron microscopy. A Gatan 666 parallel electron energy loss spectrometer was used for chemical analysis.

III. Results and Discussion

The thin film orientation on the unspattered region of the substrate is $\text{YBa}_2\text{Cu}_3\text{O}_{7-x}$ [001]//MgO [001] and $\text{YBa}_2\text{Cu}_3\text{O}_{7-x}$ [110]//MgO [110] (see figure 2). On the region which is preirradiated the orientation relation was $\text{YBa}_2\text{Cu}_3\text{O}_{7-x}$ [001]//MgO [001] and $\text{YBa}_2\text{Cu}_3\text{O}_{7-x}$ [110]//MgO [100]. Therefore a grain boundary junction is created where the irradiated and unirradiated portions of the substrate join. A few individual grains (<5% of the grain region) were unrotated on the premilled region. The junction region had both orientations intermixed across a 2 µm wide

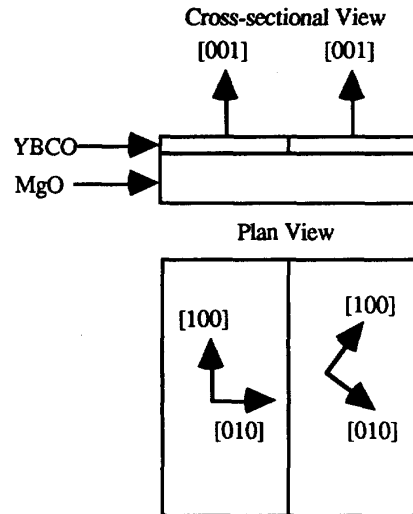


Fig. 2. Schematic of thin film orientation after deposition.

area and thus was not one pristine grain boundary.

The transport characteristics of a grain boundary junction are shown in figure 3. The junction shows typical weak link behavior with a significantly reduced critical current density relative to the adjacent grains. Figure 3 gives the voltage-current characteristics as a function of temperature from 4.2K to 77K. The critical current densities vary from 1.4×10^4 A/cm² at 4.2K to 3×10^2 A/cm² at 77K. The typical $I_c R_n$ product at 4.2K is 40µV. This value is lower than other 45° grain boundary junctions, despite relatively high critical current densities, due to the particularly low normal

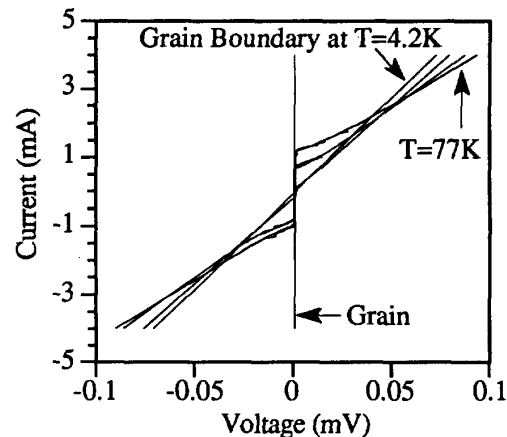


Fig. 3. Voltage-current characteristics of a grain boundary junction as a function of temperature. The temperatures shown are 4.2K, 30K, 60K and 77K. The horizontal line is the adjacent grains's characteristics.

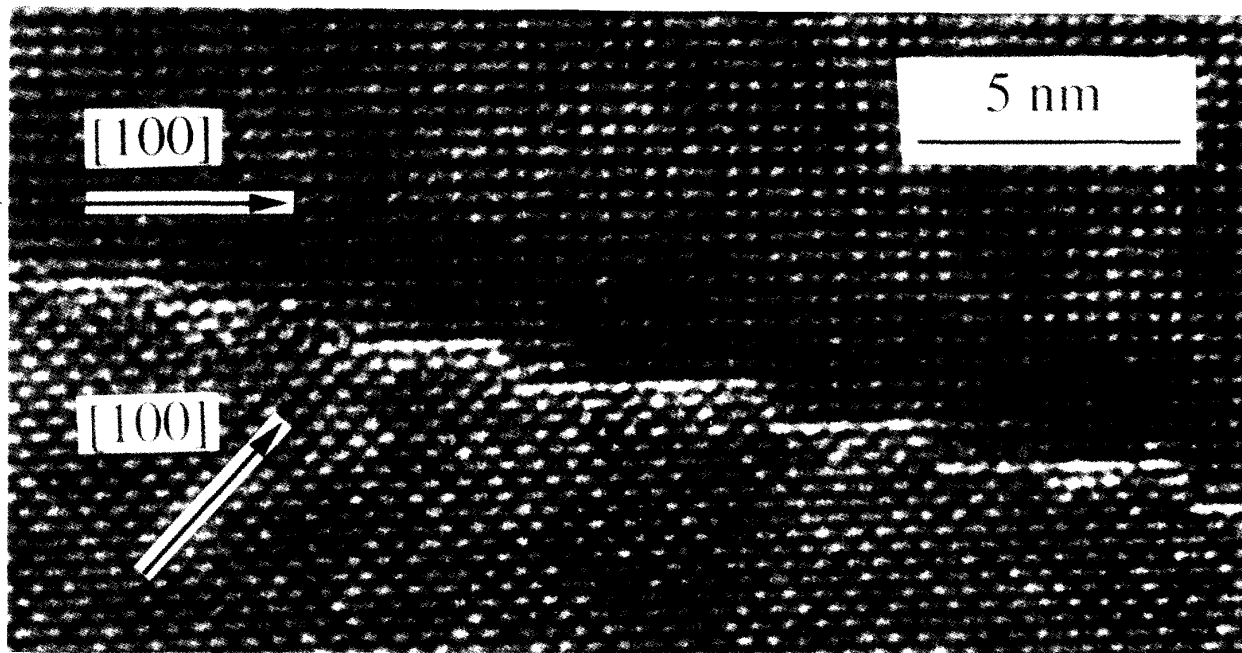


Figure 5. High resolution electron micrograph of a $\text{YBa}_2\text{Cu}_3\text{O}_{7-x}$ 45° [100] tilt grain boundary junction showing a series of asymmetric microfacets.

state resistivity $1.75\text{m}\Omega\text{-cm}$. The junction demonstrates typical resistively-shunted-junction like behavior. The dependence of the critical current density is plotted in figure 4. The data is fit to a simple model given by $J_c = J_c(0)(1 - T/T_c)^2$ [10]. The discrepancies between the data and the power-law fit probably arise from inhomogeneities along the grain boundaries. There is a strong dependence of the critical current density upon applied magnetic field which is discussed elsewhere [11].

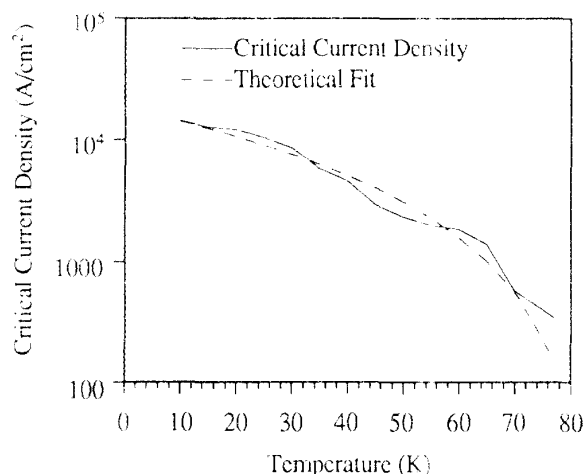


Fig. 4. The critical current density of a grain boundary junction as a function of temperature.

A high resolution electron micrograph of a grain boundary junction is shown in figure 5. The grain boundary is well structured up to the grain boundary plane. All the microfacets are straight and asymmetric on the ledges with the (100) planes of the top grain being parallel to the (110) planes of the lower grain. The asymmetry reverses at the steps where the (110) planes of the top grain are parallel to the (100) planes of the lower grain. Throughout the sample these asymmetric facets are observed, often extending several hundred angstroms in length. There are no second or amorphous phases seen along the grain boundary. The strong structural connection between the two grains is consistent with the good transport properties observed. We speculate that these straight facets form due to the extremely slow growth conditions and the presence of the oxygen plasma which allows deposition closer to equilibrium values. The well-structured boundary shows that structural distortions can be smaller than the coherence length in the a-b plane which is approximately 1.5nm. The distortion extends only up to one plane in each grain or at most 0.8nm. This implies that the weak link behavior stems either from local deviations from stoichiometry or due to inelastic scattering processes at the grain boundary. The local symmetry of the grain boundary is probably important, studies have shown that the oxygen concentration variation is smaller across symmetric grain boundaries than across asymmetric grain boundaries [12], [13]. Unfortunately these measurements could not be connected to transport properties due to the microscopic variations preventing isolation of individual microfacets of

the grain boundary. Parallel electron energy loss spectroscopy was performed across and along a grain boundary to determine the local oxygen concentration. The results showed a depletion at the grain boundary, but no variation in the stoichiometry along the grain boundary. This ensures uniformity of oxygen along the grain boundary to within the probe size of 15 Å.

This technique to reproducibly form grain boundary junctions has significant advantages over the other types of junctions currently used. The process is very simple to implement and forms planar junctions which could conceivably be used in multilayer devices. The placement of the junctions is versatile and can be used in virtually any configuration. We have grown samples with 5µm wide parallel strips with alternating grain orientations. This is a tremendous advantage over the bi-crystal junctions which are fixed in location. The MgO substrate also offers favorable high-frequency characteristics compared to other traditional substrates.

IV. Conclusions

A technique has been developed to reproducibly form 45° [001] grain boundary junctions in $\text{YBa}_2\text{Cu}_3\text{O}_{7-x}$ thin films grown on (100) MgO substrates. A low voltage Argon ion sputter pre-treatment induces a rotation in the epitaxial orientation of the film during growth. These grain boundary junctions have favorable transport properties demonstrating typical weak link behavior. Atomic level imaging shows well-structured grain boundaries with very little distortion. The boundaries are devoid of second or amorphous phases and are asymmetrically faceted. The combination of good morphology and transport properties as well as the simplicity and versatility of the technique make this an attractive method for forming grain boundary junctions.

Acknowledgment

The use of the Hitachi HF-2000 high resolution analytical electron microscope at Northwestern University is gratefully acknowledged. The use of the JEOL 4000 EXII at

Argonne National Laboratory is gratefully acknowledged.

References

- [1] P. Chaudhari, J. Mannhart, D. Dimos, C. C. Tsuei, J. Chi, M. M. Opreysko, and M. Scheuermann, "Direct Measurement of the Superconducting Properties of Single Grain Boundaries in $\text{YBa}_2\text{Cu}_3\text{O}_{7-x}$," *Phys. Rev. Lett.*, vol. 60, pp. 1653-1656, 1988.
- [2] D. Dimos, P. Chaudhari, J. Mannhart, and F. K. LeGoues, "Orientation dependence of grain-boundary critical currents in $\text{YBa}_2\text{Cu}_3\text{O}_{7-x}$ bicrystals," *Phys. Rev. Lett.*, vol. 61, pp. 219-222, 1988.
- [3] Z. G. Ivanov, P. Å. Nilsson, D. Winkler, J. A. Alarco, T. Claeson, E. A. Stepanov, and A. Y. Tzalenchuk, "Weak links and dc SQUIDs on artificial nonsymmetric grain boundaries in $\text{YBa}_2\text{Cu}_3\text{O}_{7-x}$," *Appl. Phys. Lett.*, vol. 59, pp. 3030-3032, 1991.
- [4] D. Dimos, P. Chaudhari, and J. Mannhart, "Superconducting transport properties of grain boundaries in $\text{YBa}_2\text{Cu}_3\text{O}_{7-x}$ bicrystals," *Phys. Rev. B*, vol. 41, pp. 4038-4049, 1988.
- [5] K. Char, M. S. Colclough, S. M. Garrison, N. Newman, and G. Zaharchuk, "Bi-epitaxial grain boundary junctions in $\text{YBa}_2\text{Cu}_3\text{O}_{7-x}$," *Appl. Phys. Lett.*, vol. 59, pp. 733-735, 1991.
- [6] K. Char, M. S. Colclough, L. P. Lee, and G. Zaharchuk, "Extension of the bi-epitaxial Josephson junction process to various substrates," *Appl. Phys. Lett.*, vol. 59, pp. 2177-2179, 1991.
- [7] C. L. Jia, B. Kabius, K. Urban, K. Herrmann, G. J. Cui, J. Schubert, W. Zander, A. I. Braginski, and C. Heiden, "Step edges in $\text{YBa}_2\text{Cu}_3\text{O}_{7-x}$ thin films," *Physica C*, vol. 175, pp. 543, 1991.
- [8] N. G. Chew, S. W. Goodyear, R. G. Humphreys, J. S. Satchell, J. A. Edwards, and M. N. Keene, "Orientation control of $\text{YBa}_2\text{Cu}_3\text{O}_{7-x}$ thin films on MgO for epitaxial junctions," *Applied Physics Letters*, vol. 60, pp. 1516-1518, 1992.
- [9] D. B. Buchholz, S. J. Duray, D. L. Schulz, T. J. Marks, J. B. Ketterson, and R. P. H. Chang, "Surface morphology studies of Y-Ba-Cu-oxide thin films prepared by pulsed organometallic beam epitaxy," *Materials Chemistry and Physics*, vol. 36, pp. 377-382, 1994.
- [10] R. Gross, "Grain boundary Josephson junctions in the high temperature superconductors," in *Interfaces in superconducting systems*, S.L. Shinde and D. Rudman, Eds. New York: Springer Verlag, 1992, pp. 1-47.
- [11] B. V. Vuchic, K. L. Merkle, K. A. Dean, D. B. Buchholz, R. P. H. Chang, and L. D. Marks, "Sputter-induced grain boundary junctions in $\text{YBa}_2\text{Cu}_3\text{O}_{7-x}$ thin films on MgO," to be published *Journal of Applied Physics*.
- [12] N. D. Browning, M. F. Chisholm, and S. J. Pennycook, "Cell-by-cell mapping of carrier concentrations in high-temperature superconductors," *Interface Science*, vol. 1, pp. 309-319, 1993.
- [13] Y. Zhu, Z.L. Wang, and M. Suenaga, "Grain-boundary studies by the coincident-site lattice model and electron-energy-loss spectroscopy of the oxygen K edge in $\text{YBa}_2\text{Cu}_3\text{O}_{7-x}$," *Philosophical Magazine A*, vol. 67, pp. 11-28, 1993.